2018

Ignition Studies of Oxy-Syngas/CO2 Mixtures Using Shock Tube for Cleaner Combustion Engines

Samuel Barak
University of Central Florida

IGNITION STUDIES OF OXY-SYNGAS/CO2 MIXTURES USING SHOCK TUBE FOR CLEANER COMBUSTION ENGINES

by

SAMUEL EVAN BARAK
B.S. University of Florida, 2015

A thesis submitted in partial fulfillment of the requirements
for the degree of Master of Science
in the Department of Mechanical and Aerospace Engineering
in the College of Engineering and Computer Science
at the University of Central Florida
Orlando, Florida

Spring Term
2018

Major Professor: Subith Vasu

ABSTRACT

In this study, syngas combustion was investigated behind reflected shock waves in order to gain insight into the behavior of ignition delay times and effects of the CO2 dilution. Pressure and light emissions time-histories measurements were taken at a 2 cm axial location away from the end wall. High-speed visualization of the experiments from the end wall was also conducted. Oxy-syngas mixtures that were tested in the shock tube were diluted with CO2 fractions ranging from 60% - 85% by volume. A 10% fuel concentration was consistently used throughout the experiments. This study looked at the effects of changing the equivalence ratios (ϕ), between 0.33, 0.5, and 1.0 as well as changing the fuel ratio (θ), hydrogen to carbon monoxide, from 0.25, 1.0 and 4.0. The study was performed at 1.61-1.77 atm and a temperature range of 1006-1162K. The high-speed imaging was performed through a quartz end wall with a Phantom V710 camera operated at 67,065 frames per second. From the experiments, when increasing the equivalence ratio, it resulted in a longer ignition delay time. In addition, when increasing the fuel ratio, a lower ignition delay time was observed. These trends are generally expected with this combustion reaction system. The high-speed imaging showed non-homogeneous combustion in the system, however, most of the light emissions were outside the visible light range where the camera is designed for. The results were compared to predictions of two combustion chemical kinetic mechanisms: GRI v3.0 and AramcoMech v2.0 mechanisms. In general, both mechanisms did not accurately predict the experimental data. The results showed that current models are inaccurate in predicting CO2 diluted environments for syngas combustion.

ACKNOWLEDGMENTS

Firstly, I would like to thank my fiancé *Danielle Lehrer* for her love, support, affection, and patience throughout my time during this program. I would also like to thank my parents *Alex and Raquel Barak* for leading me on this path from an early age, teaching me the value of education and working hard for what you want.

I would like to thank my advisor *Dr. Subith Vasu* for all the guidance, support, and knowledge he has given me over the last two and a half years; as well as, my committee members *Dr. Jayanta Kapat* and *Dr. Kareem Ahmed* for their roles associated.

I would also like to thank all my colleagues from the University of Central Florida; especially those within the Shock Tube Group, for teaching me how to use the shock tube and assisting me in performing the research in this thesis. Additionally, I would like to thank *Bob Wong* for his machining expertise that has been crucial to continuing the operation of my experiments.

This work was supported by the Department of Energy, American Chemical Society Petroleum Research Fund and the Defense Threat Reduction Agency.

TABLE OF CONTENT

LIST OF FIGURES vii

LIST OF TABLES viii

NOMENCLATURE ix

CHAPTER ONE: INTRODUCTION 1

CHAPTER TWO: EXPERIMENTAL METHODS 3

Shock Tube System 3

Mixture Preparation 4

Ignition Delay Time Measurements 4

High-Speed Imaging 5

Replication Setup 6

CHAPTER THREE: RESULTS AND DISCUSSION 7

Replication Study 7

CHAPTER FOUR: OBSERVATIONS 8

High-Speed Image Processing 8

Ignition Delay Times of Replication Study 9

Increased CO_2 Dilution in Syngas Mixtures 10

Change of the Equivalence Ratio ϕ 15

Change of the Hydrogen-to-Carbon Monoxide Ratio, θ 20

CHAPTER FIVE: CONCLUSIONS 24

REFERENCES 26

LIST OF FIGURES

Figure 1. Pressure trace of replication study including emissions detector and camera emissions.9
Figure 2. The data points with 20% uncertainty in our study compared to the provided data points in [4]. 10
Figure 3. Pressure trace of an experiment using mixture 2 including emissions detector and camera emissions. 11
Figure 4. These images were from the experiment plotted in Figure 3. Image (A) refers to the end wall emissions at 943.92 μs. The slope method determined ignition at 947 μs. Image (B) refers to the end wall emissions at 1286.85 μs. The peak method determined ignition at 1288 μs. An artificial ring was placed to show the circumference of the shock tube. 12
Figure 5. Mixture 2 experimental data points with 20% uncertainty are compared with two combustion kinetic models. 13
Figure 6. Pressure trace of an experiment using mixture 3 including emissions detector. 13
Figure 7. Ignition delay time comparison between mixture 2 and mixture 3 experiments. 14
Figure 8. Pressure trace of an experiment using mixture 4 including emissions detector and camera emissions. 15
Figure 9. These images were from the experiment plotted in Figure 8. Image (A) refers to the end wall emissions at 72.23 μs. The slope method determined ignition at 78 μs. Image (B) refers to the end wall emissions at 176.6 μs. The peak method determined ignition at 176 μs. An artificial ring was placed to show the circumference of the shock tube. 16
Figure 10. Pressure trace of an experiment using mixture 5 including emissions detector and camera emissions. 17
Figure 11. These images were from the experiment plotted in Figure 10. Image (A) refers to the end wall emissions at 239.24 μs. The slope method determined ignition at 245 μs. Image (B) refers to the end wall emissions at 343.61 μs. The peak method determined ignition at 340.5 μs. An artificial ring was placed to show the circumference of the shock tube. 18
Figure 12. A plot of mixtures 3, 4 and 5 experiments. A change of ϕ resulted in differences in ignition delay time. These plots are compared to GRIMech v3.0 and AramcoMech V2.0. . 19
Figure 13. Pressure trace of an experiment using mixture 6 including emissions detector and camera emissions. 21
Figure 14. Pressure trance of an experiment using mixture 7 including the emissions detector. . 21
Figure 15. A plot of mixtures 3, 6 and 7 experiments. A change of θ resulted in differences in ignition delay time under similar conditions. 22

LIST OF TABLES

Table 1. The mixtures that were experimented with and presented in this paper..... 7

NOMENCLATURE

Ar	Argon
CO_2	Carbon Dioxide
CO	Carbon Monoxide
Φ	Equivalence Ratio
OH*	Excited hydroxyl radical
Θ	Fuel Ratio of Hydrogen to Carbon Monoxide
H_2	Hydrogen
OH	Hydroxyl radical
IDT	Ignition Delay Time
O_2	Oxygen
UV	Ultraviolet

CHAPTER ONE: INTRODUCTION

There is an increasing demand for energy in the industrialized world. Trends have shown that people are interested in cleaner energy production. Most of power generation comes from burning fuels for energy in power plants across the world. This results in greenhouse gas emissions and other undesirable pollutants. There is development in power generation technology that looks to improvement on cycle efficiencies. Current technology has stretched the efficiencies of supercritical steam cycles and the use of supercritical CO_2 in power cycles can improve efficiencies even further. However, there is much to be developed before full operations with supercritical CO_2 power cycles can begin. Another benefit of a supercritical CO_2 cycle is that it will eliminate NOx emissions that results from combustion in air due to the CO_2 cycle being closed. This novel design, directly heated combustion in supercritical CO_2 with combined CCS (carbon capture and storage), is being developed by National Energy Technology Laboratory (NETL) and private industry [1, 2].

Synthesis gas, or syngas, is a fuel resulting from gasification of coal or biomass that offers the potential for cleaner burning in a power plant. A simplified model of syngas is a fuel primarily consisting of hydrogen and carbon monoxide. It has been demonstrated [3] that syngas composition is widely variable as well, complicating the design of the gas turbines. A need for experiments with a change in θ is needed as gasification results in varied fuel composition from location and processes [4]. Studies have been done to measure the ignition delay times of various compositions of oxy-syngas combustion in air, [4, 5], however, very little has been done to see the effects that CO_2 has on the combustion process. Some studies [6-8] examined the effects of CO_2 diluted syngas at a CO_2 concentration up to 30% CO_2. Furthermore [9, 10] examined the

effects of CO_2 on oxy-methane combustion at dilution up to 60% and observed an increase in ignition delay time. Therefore, it is unknown of the effects of high concentrations of CO_2 on syngas combustion and experimentation must be done.

This study examines the ignition delay time of oxy-syngas combustion in a shock tube with CO_2 dilutions from 60%-85%. This study looked at the effects of changing ϕ, the equivalence ratio, from 0.33-1.0 as well as changing θ, the fuel ratio of hydrogen to carbon monoxide, from 0.25-4.0. The study was performed at 1.61-1.77 atm and a temperature range of 1006-1162K. The experimental data was compared with two combustion chemical kinetic mechanisms GRI-Mech v3.0 [11] and AramcoMech v2.0 [4]. In addition, high-speed imaging of the experiments was taken at the end wall of the shock tube to compare with different methods of determining the ignition delay time.

CHAPTER TWO: EXPERIMENTAL METHODS

Shock Tube System

All of the experiments of this study were taken with a stainless-steel shock tube. This shock tube has an inner diameter of 14.17 cm. The driver side is filled with helium and separated by a polycarbonate Lexan diaphragm. The driven side is filled to a specified pressure with a mixture prepared in a separate tank. When this diaphragm ruptures, a shock wave is formed and quickly travels down the driven side of the shock tube and heats up the test mixture. Five piezoelectric pressure transducers (PCB 113B26) placed along the last 1.4 m of the shock tube were used to measure the incident shock wave velocity using four time-interval counters (Agilent 53220A). The incident shock wave attenuation was always less than 1%. With the known velocity and a measured initial temperature and pressure of the driven side, one dimensional ideal shock relations can be used to calculate the reflected shock wave temperatures and pressures [12]. Data was recorded using a NI PCI-6133 Data Acquisition Device at 2MHz per channel. Measurements were taken radially at a test section 2 cm from the driven side end wall that contains eight optical ports. One of the ports has a piezoelectric pressure transducer (Kistler 603B1) to measure the pressure in the driven section. Another port contained a GaP transimpedance amplified detector (Thorlabs PDA25K) operating in the wavelength range between 150 and 550 nm. This detector is used to measure the emissions of combustion (mostly OH*). No filters were placed in front of this detector to achieve a high signal-to-noise ratio. A continuous wave laser detailed in [9, 13-15] was used only to determine time-zero by the laser schlieren spike of the arrival of the reflected shock wave at the measurement location.

Mixture Preparation

Before each set of shock tube experiments, a mixture was prepared in a 33-liter Teflon-coated stainless steel mixing tank. Each mixture was prepared by vacuuming the mixing tank to at least 5 x 10^{-5} Torr using a turbo molecular pump (Agilent model V301) in conjunction with rotary vane pumps (Agilent DS102). Vacuum pressures were measured using a convection (Lesker KJL275804LL) and ionization (Lesker KJLC354401YF) gauges. Mixtures were made from research grade gasses supplied by Praxair, Inc. The pressure was measured using a 100 Torr (MKS Instruments Baratron E27D) and a 10,000 Torr (MKS Instruments/Baratron 628D) full scale range capacitance type manometers. Each gas was introduced into the mixing tank and the use of partial pressures were used to determine mole fractions. The mixtures were then mixed for at least eight hours using a magnetically driven stirrer to ensure homogeneity.

Ignition Delay Time Measurements

The ignition delay time measurement of the shock tube was defined as the time interval between the arrival of the reflected shockwave and the onset of the ignition at the measurement location. The arrival, or time zero, was determined by the laser schlieren spike of a continuous wave beam cascade laser. The onset of the ignition time was determined by evaluating the time-history of the emissions, finding the steepest rise, and then extrapolating down to the baseline measurement. This method was described in a previous study [16]. This ignition delay time was compared with the high-speed imaging of the combustion event. These measurements were also compared with the predictions of two different reaction mechanisms, GRIMech 3.0 [11] and

AramcoMech 2.0 [4]. The mechanisms were used on CHEMKIN PRO [17] using constant-volume, internal energy (constant V, U) assumption and results were compiled. Constant V, U assumption has been used on similar shock tube combustion studies [4-7] and with CO_2 dilution [6, 9, 18]. In CHEMKIN PRO, the ignition delay time was calculated with a similar method for calculating the ignition delay time as the shock tube experiments by using the OH concentration time-history. The steepest rise in this plot was then extrapolated down to the baseline measurement to determine the ignition delay time. OH concentration was used due to its major importance during ignition. It should be pointed out that the simulations with another ignition delay time definition, which is based on the temperature inflection point, matched fairly well (within <1%) with the ones obtained from the OH concentrations.

High-Speed Imaging

High-speed imaging of the shock tube was taken using a Phantom V710 camera. This camera has a 1280x800 CMOS sensor that is adjustable with the computer program Phantom Camera Control Application (PCC) to 256x256 resolution at 67,065 frames per second. The camera is then able to take an image every 14.91 μs with an exposure time of 14.467 μs. The output of the camera is in greyscale. The camera program is turned on during the experiment and uses a triggering mechanism by a wired input into the Kistler pressure trace voltage. Using the camera capturing program, the trigger waits until a rising edge of at least 2 volts for 5 μs is detected to determine time-zero for the camera. Samples before and after the triggering event are then saved and evaluated. The camera is placed 2.13 meters perpendicular from the end wall in order to view the entire diameter of the shock tube and is focused at the 2cm location of the other measurements. A Fused Quartz end wall replaced the original stainless-steel end wall to allow

transparency. The camera is then able to observe ignition events down the entire length of the shock tube. The shock tube was cleaned frequently to avoid diaphragm particles from impacting images significantly. The images are post-processed on Matlab and the emissions are indexed in a matrix, normalized to the brightest image. A false-color heat map is applied to each image and an artificial circle is placed on the images to note the shock tube diameter. A camera emissions plot is then evaluated using the peak of the GaP transimpedance amplified detector and included in the plots of the data collection. Further details of this setup and details of the plot being normalized to the emissions detector can be found in [18].

Replication Setup

In order to validate our shock tube for syngas experiments, a study was done to replicate a set of experiments performed in [4]. The measurement for ignition delay time were described as the time between the initiation of the system by the reflected shock wave and the occurrence of the [OH] maximum. The replicated tests were the data points at 1 atm.

CHAPTER THREE: RESULTS AND DISCUSSION

Table 1. The mixtures that were experimented with and presented in this paper.

Table 1: Reactant Mixtures Investigated							
Mixture	ϕ	θ	% H_2	% CO	% O_2	% CO_2	% Ar
1	0.5	1.02	1.75	1.72	3.47	0	93.06
2	0.5	1.00	5	5	10	60	20
3	0.5	1.00	5	5	10	80	0
4	0.33	1.00	5	5	15	75	0
5	1.00	1.00	5	5	5	85	0
6	0.5	4.00	8	2	10	80	0
7	0.5	0.25	2	8	10	80	0

All of the mixtures of experiments presented can be found in Table 1. It begins with the replication study mixture. The rest of the mixtures capture the change of ϕ from 0.33-1.0. It also covers a change of θ from 0.25-4.0.

Replication Study

Ignition delay time measurements were taken to replicate a study in [4]. The mixture that was created was slightly different from that study. The study had a θ value of 1.0, while the mixture I made was 1.02. In both mixtures, a ϕ of 0.5 was consistent.

CHAPTER FOUR: OBSERVATIONS

High-Speed Image Processing

The high-speed imaging provides insight into the homogeneity of combustion in the shock tube to compare to standard methods (e.g. pressure, emissions) which assume homogenous ignition. The light sources from this reaction are from the oxy-hydrogen flame and the carbon monoxide oxidation flame. The oxy-hydrogen flame emits light primarily from 200 nm to 400 nm range, mainly due to strong OH band emissions at 306.36nm, 306.76nm and 309.04nm [19]. The carbon monoxide oxidation flame primarily is in the 350nm to 450 nm range, due to forming CO_2 emissions at 402.6 nm [19], however, is heavily driven by OH formation. The camera used, the Phantom V710, was designed to operate in the visible light range, 390 nm - 700 nm. The quantum efficiency (ie: the effectiveness of the camera to see light at a specific wavelength) quickly declines at lower wavelengths and is reported to be 15% at 350 nm [20]. Below this value, the efficiency was not recorded by the manufacturer. Even considering the broadening of emissions due to increases in temperature and pressure, the emissions are in wavelengths below the camera's design parameter. The emissions detector is designed to see light emissions from 150 nm to 550 nm. Signal intensity was very low when a bandpass filter was placed in front of the detector because CO2 dilution makes emission intensity significantly go down. Therefore, no filter was used. When ignition starts, the concentrations of the radicals (eg. OH) make a peak. The intensity of the emission is directly proportional to the number density of the OH molecules, which is not captured by the camera operating in the visible light. After the radical concentration makes a peak, there is a dramatic decrease in fuel concentration due to the reactions between those radicals and other molecules. Since the camera cannot detect light in the UV range, the

images recorded correspond to a time slightly later than onset of ignition. Therefore, only images at the onset of combustion until the peak of emissions determined from the emissions detector are considered.

Ignition Delay Times of Replication Study

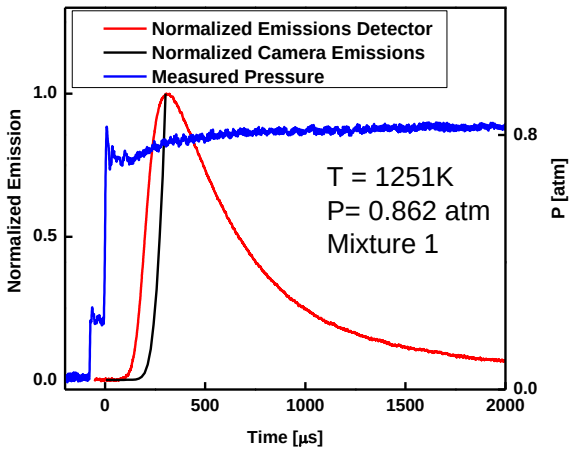

FIGURE 1. Pressure trace of replication study including emissions detector and camera emissions.

Figure 1 is a single experiment pressure trace of the replication study done. The main combustion event does not provide a large change in the pressure of the system. Also, included with the pressure are the normalized emissions detector trace as well as the normalized camera emissions. The camera emissions are slightly behind the emissions detector due to it being unable to see OH emissions. The same method for calculating the ignition delay time using the peak of emissions was used as described in the study.

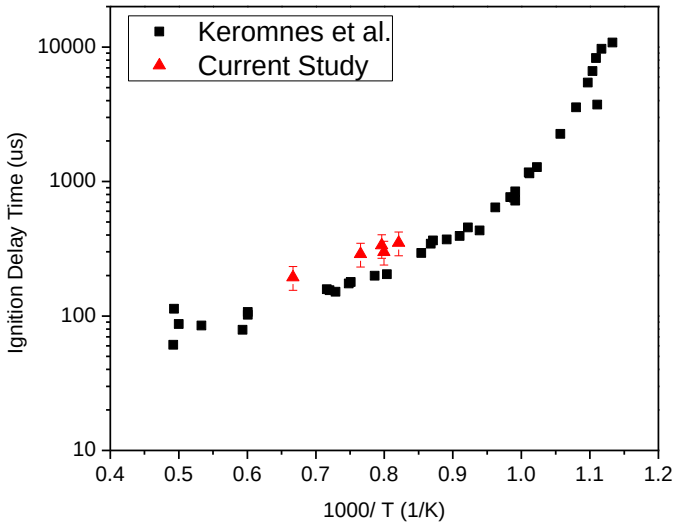

FIGURE 2. The data points with 20% uncertainty in our study compared to the provided data points in [4].

As seen in Figure 2, the data points of our study were at slightly higher ignition delay times compared with the data points of the previous study, however, the trends are similar and the differences are within the limits of the uncertainties of the measurements. There were a few differences in the mixture that were noted previously.

Increased CO_2 Dilution in Syngas Mixtures

Mixtures 2 and 3 have similar fuel and oxygen compositions, however; mixture 2 has 60% CO_2 dilution compared to the 80% CO_2 dilution in mixture 3. Bifurcation of the shock wave due to the CO_2 dilution is noticeable in the pressure traces in between the incident and reflected shocks of the experiment as well the other mixtures of this paper. This phenomenon is properly documented for these dilutions [9, 18].

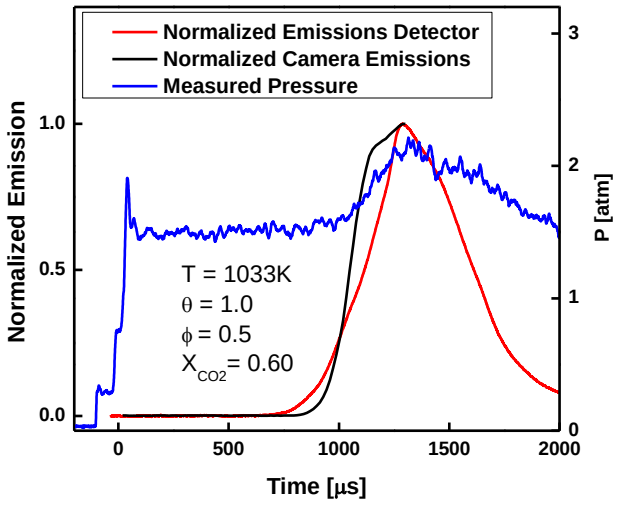

FIGURE 3. Pressure trace of an experiment using mixture 2 including emissions detector and camera emissions.

Figure 3 is a pressure trace of 60% CO_2 experiment. A clear pressure rise is seen in the experiment that matches the emissions detector. The high-speed camera was able to capture the ignition event as well. The end wall emissions from the camera are slightly behind compared to the emissions detector, however, it eventually observes more light (down the length of the shock tube) than the detector as evident of the steeper rise of the slope compared to the camera emissions.

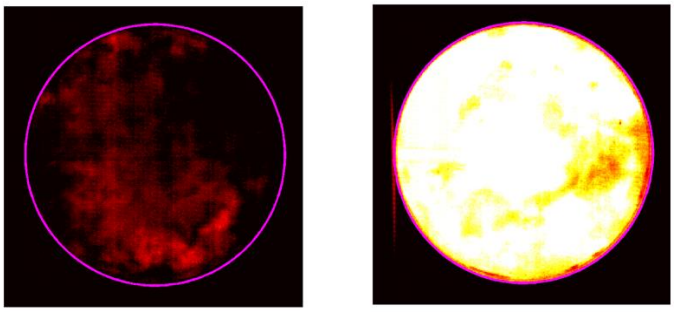

FIGURE 4. These images were from the experiment plotted in Figure 3. Image (A) refers to the end wall emissions at 943.92 μs. The slope method determined ignition at 947 μs. Image (B) refers to the end wall emissions at 1286.85 μs. The peak method determined ignition at 1288 μs. An artificial ring was placed to show the circumference of the shock tube.

Using two methods for determining ignition delay time Figure 4 shows images of the flame using both the slope method (A) and a bright image at the peak of emissions (B). At the peak of emissions, a completely homogenous combustion event is observed throughout the entire shock tube cross section.

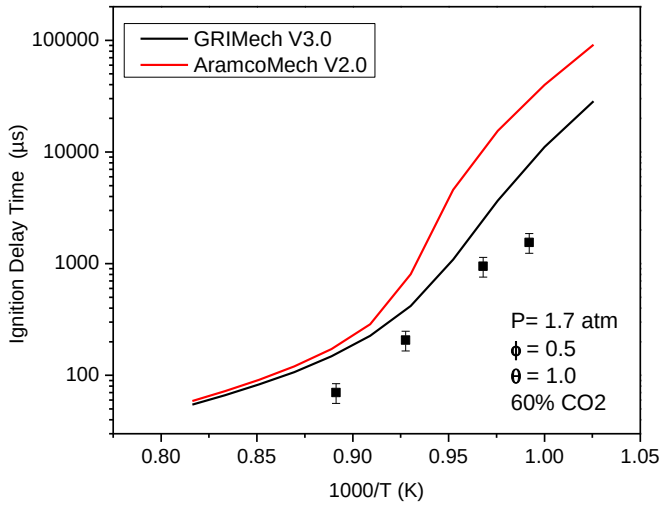

FIGURE 5. Mixture 2 experimental data points with 20% uncertainty are compared with two combustion kinetic models.

The data points collected using the slope method are compared with two combustion chemical kinetic mechanisms in Figure 5. The data does not match up well with these predictions, however, follow a similar trend.

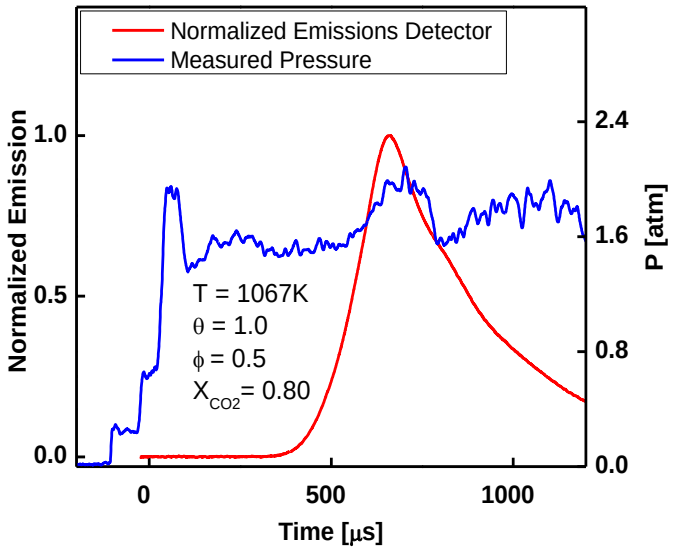

FIGURE 6. Pressure trace of an experiment using mixture 3 including emissions detector.

Figure 6 is a pressure trace of an 80% CO_2 experiment where ϕ =0.5. A pressure rise is visible at the same time as the emissions detector. No camera data was taken of this mixture for comparison. The chemical kinetic mechanisms were compared to these experiments of mixture 3 and are presented at a later part in this paper.

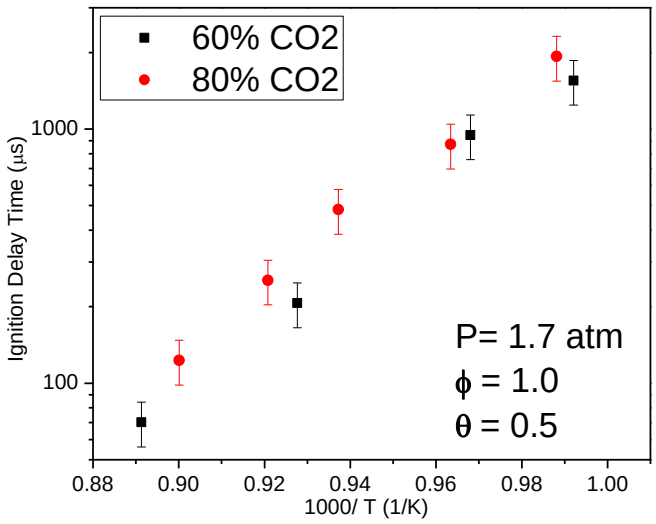

FIGURE 7. Ignition delay time comparison between mixture 2 and mixture 3 experiments.

It is expected that with an increase in CO_2 amount, from mixture 3, an increase in the ignition delay time was observed. The primary reactions that are impacted are as followed:

$$CO + OH \rightleftharpoons CO_2 + H \qquad (R1)$$

$$H + O_2 \rightleftharpoons O + OH \qquad (R2)$$

It has been observed that CO_2 is not an inert bath gas in the ignition of syngas combustion. CO_2 competes for the H radicals through the reverse reaction of R1, which results in a decrease in the concentration of the H radicals that participates in the chain branching reaction given by R2. This is consistent with previous observations [21] of the chemical effect of CO_2 on

methane and hydrogen flames. In the same shock tube facility, similar observations were confirmed utilizing methane as the fuel instead of syngas [9, 18].

Although within the uncertainty of the experiments from figure 7 that compares the ignition delay time for mixtures 2 and 3, it is expected that an increase in CO_2 concentration increases the ignition delay time for the same oxy-syngas composition at these test conditions. The purpose was to study syngas combustion in CO_2 dilution and compare these with current chemical kinetic models. It will be shown throughout this publication that the ignition delay times are lower than the models predictions, due to the CO_2 interaction.

Change of the Equivalence Ratio ϕ

ϕ was changed between 0.33, 0.5, and 1 (mixtures 4, 3, and 5, respectively).

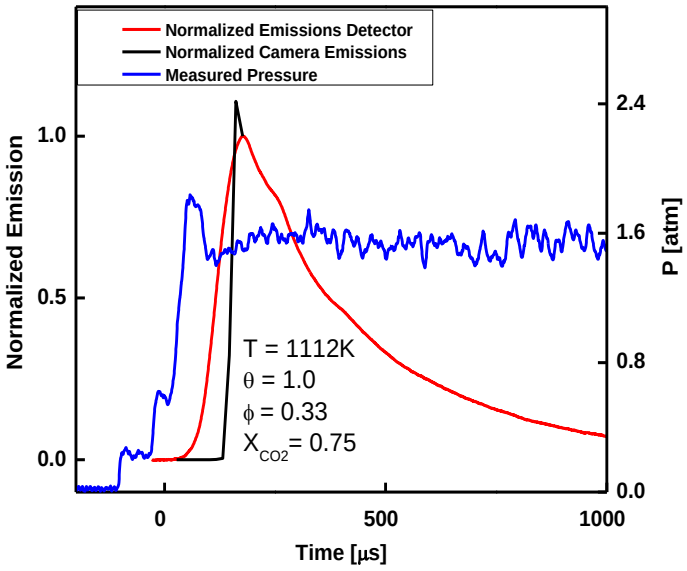

FIGURE 8. Pressure trace of an experiment using mixture 4 including emissions detector and camera emissions.

Figure 8 is a pressure trace of an experiment with a ϕ of 0.33 in mixture 4. The fuel lean mixture 4 did not exhibit a pressure rise typically seen with combustion. A similar observation was seen for CO_2 diluted mixtures in methane and [10, 18]. The measurement results quantified using the camera images initially fell behind those of the emissions detector. However, more light was observed from the camera measurements downstream of the tube, resulting in a higher maximum intensity. This was seen since the normalized camera emissions were greater than unity at a time before the peak of the emissions detector at the 2 cm location.

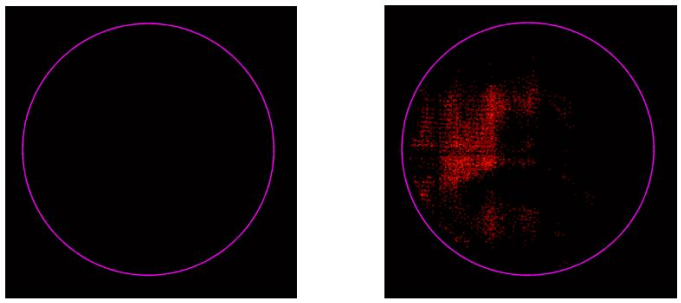

FIGURE 9. These images were from the experiment plotted in Figure 8. Image (A) refers to the end wall emissions at 72.23 μs. The slope method determined ignition at 78 μs. Image (B) refers to the end wall emissions at 176.6 μs. The peak method determined ignition at 176 μs. An artificial ring was placed to show the circumference of the shock tube.

The images of combustion in Figure 9 show non-homogenous combustion with a very weak flame event. Compared to Figure 4B, where the combustion event consumes the entire cross section of the shock tube, this was not observed for this mixture at important ignition times. Bifurcation of the shock due to the CO_2 dilution has been previously observed with high-speed

imaging to disrupt the homogeneity of the shock wave during ignition [18, 22]. This effect is increased with higher CO_2 dilutions. In Figure 9, the camera failed to detect light at the time of ignition determined by the slope method (A), but observed light at the time of the peak of emissions (B).

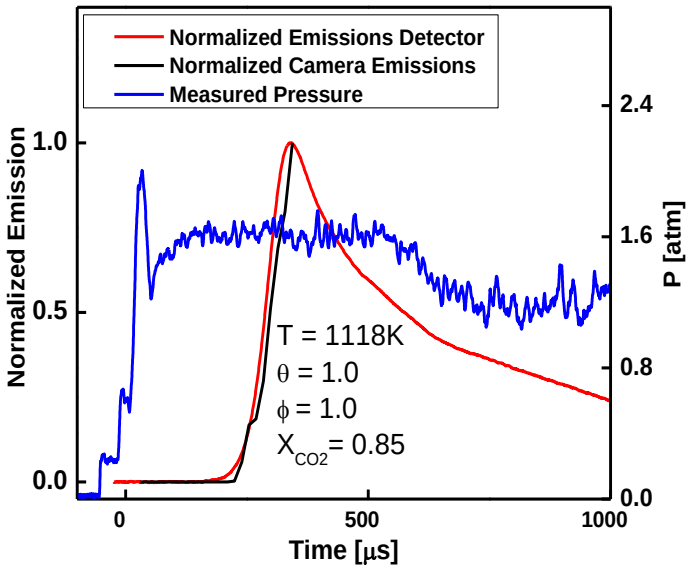

FIGURE 10. Pressure trace of an experiment using mixture 5 including emissions detector and camera emissions.

Figure 10 is a pressure trace of an experiment with a ϕ of 1.0 in mixture 5. A similar temperature from Figure 8 was chosen for Figure 10 to distinguish the difference in the ignition delay time. There was not a noticeable rise in the pressure from combustion in this mixture. The camera emissions were slightly behind the emissions detector in this mixture, however, provided insight into the flame characteristics.

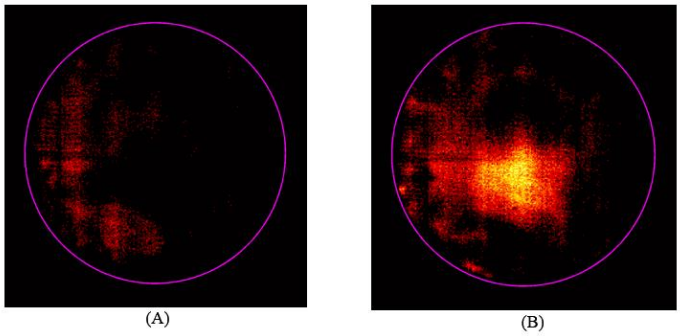

FIGURE 11. These images were from the experiment plotted in Figure 10. Image (A) refers to the end wall emissions at 239.24 μs. The slope method determined ignition at 245 μs. Image (B) refers to the end wall emissions at 343.61 μs. The peak method determined ignition at 340.5 μs. An artificial ring was placed to show the circumference of the shock tube.

In Figure 11, a flame is visible in the ϕ = 1.0 mixture 5 experiments correlating to the slope method (A) for determining the ignition delay time as well as the peak method (B). The flame is non-homogenous, similarly to the fuel lean mixture in Figure 9. The effect of CO_2 addition on the homogeneity of both the fuel lean (Figure 9) and ϕ = 1.0 (Figure 11) mixtures are apparent when compared to a lower CO_2 dilution (Figure 4).

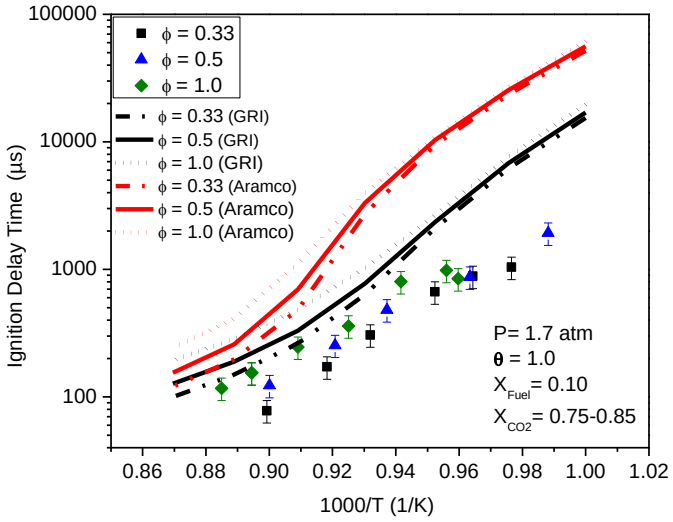

FIGURE 12. A plot of mixtures 3, 4 and 5 experiments. A change of ϕ resulted in differences in ignition delay time. These plots are compared to GRIMech v3.0 and AramcoMech V2.0.

Figure 12 compares the predictions of the two combustion chemical kinetic mechanisms with measurement results obtained using the mixtures of 3, 4 and 5. Neither models accurately predicted the ignition delay times considering a 20% uncertainty in the ignition delay time measurements. The fuel lean mixture had a shorter ignition delay time. This was primarily because of a higher concentration of free radicals including OH, which is the radical involved in the primary reaction mechanism of both hydrogen and carbon monoxide combustion (i.e. R1 and R2). Although incorrect in estimation for all three mixtures, the models did, however, have accurate trends. These trends in the temperature match previous findings [4, 5, 7], for a change in ϕ in syngas mixtures.

Change of the Hydrogen-to-Carbon Monoxide Ratio, θ

A change of the fuel ratio was also performed at a fixed equivalence ratio of $\phi = 0.5$. This allows better insight on the contributions of each fuel to combustion.

Figure 13 is a pressure trace of an experiment with a change of θ from 1.0 to 4.0 in mixture 6 compared to mixture 3. A large pressure rise was not seen during combustion with this mixture. Camera emissions matched well with the emissions detector, but with some initial delayed response.

In the experiments of mixture 7, where θ was decreased from 1.0 to 0.25, there were noticeable changes. Camera imaging was not taken for mixture 7. In Figure 14, a pressure trace is given as well as the emissions detector trace. This mixture, with a larger carbon monoxide percentage, had a slower energy release as compared to other mixtures as seen in the emissions detector. This is to be expected as carbon monoxide combustion is a much slower reaction as compared to the hydrogen combustion reaction and was previously observed [4].

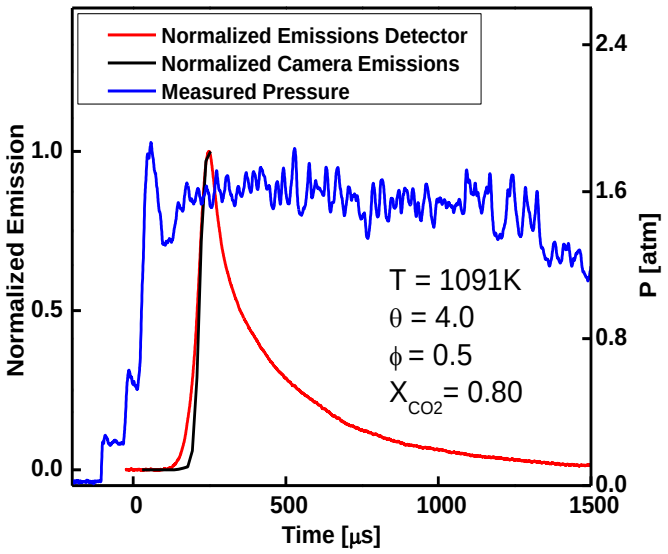

FIGURE 13. Pressure trace of an experiment using mixture 6 including emissions detector and camera emissions.

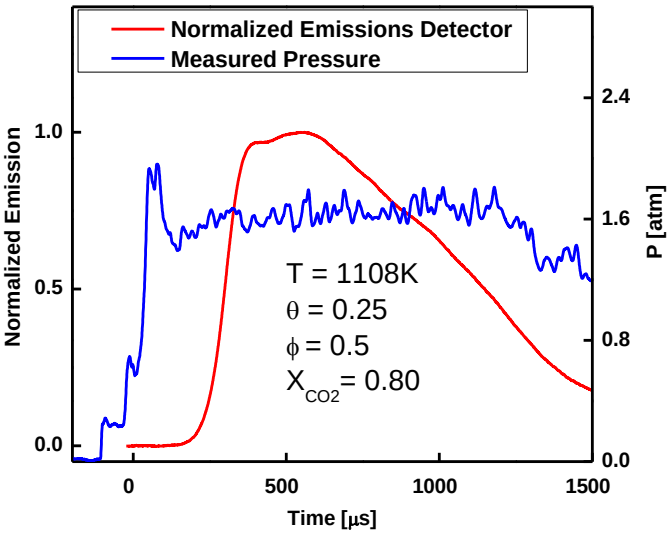

FIGURE 14. Pressure trance of an experiment using mixture 7 including the emissions detector.

For mixture 6, $\theta = 4.0$, the models did not accurately predict the trend at colder temperatures. Both models predict an increased ignition delay time at lower temperatures,

however the observed ignition delay time does not substantially change from 1000 K to 1050 K. This was observed with a θ greater than 1.0 [4, 7]. It is explained that at low temperatures competition between the chain branching reaction (R3) and chain termination reaction (R4) occur:

$$H + O_2 = OH + H \qquad (R3)$$

$$H + O_2 (+M) = HO_2 (+M) \qquad (R4)$$

The former dominates the ignition chemistry at high temperature while the latter dominates at intermediate to low temperatures [7].

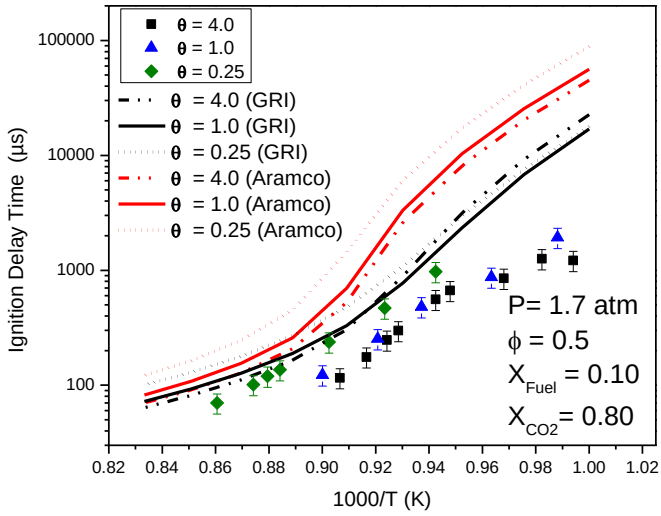

FIGURE 15. A plot of mixtures 3, 6 and 7 experiments. A change of θ resulted in differences in ignition delay time under similar conditions.

Figure 15 compares the two combustion chemical kinetic mechanisms with mixtures of 3, 6, and 7. Neither model accurately predicted the ignition delay times for the mixtures tested. The

trends in mixtures 6 and 7 are expected and match what was observed by [5, 7] for a change in θ, with a minor exception to low temperatures in the mixture with θ = 4.0.

Mixtures with a larger value of θ had a shorter ignition delay time due to the presence of more hydrogen. Hydrogen has a much faster ignition chemistry relative to those of carbon monoxide combustion (which relies on hydroxyl formation). There was a little difference in the ignition delay time of mixtures 3 and 6, where θ changes from 1.0 to 4.0. The free radical formation for both mixtures satisfied the CO reaction to form CO_2. Whereas in mixture 7, with θ = 0.25, much less hydrogen existed to be able to form necessary free radicals for the same reaction to occur, resulting in the noticeable increase in the ignition delay time. Similar observations were made in previous studies [4, 5, 7, 8, 18].

Present work highlights the importance of collecting experimental data in syngas mixtures so that kinetic mechanisms can be validated in mixtures with high CO_2 dilution. Effort is currently underway in our laboratory to expand the range of T, P, and concentrations for experiments.

CHAPTER FIVE: CONCLUSIONS

This is first comprehensive experiments on the effects of adding high levels of CO_2 to syngas ignition delay times in a shock tube. This work measured the ignition delay time of oxy-syngas combustion in a shock tube with CO_2 dilutions from 60%-85% between 1006-1162K. Different mixtures of H_2/CO were used to see the effects of changing ϕ as well as θ. The ignition delay times had a positive correlation with ϕ showing that as the equivalence ratio decreased, the ignition delay times became shorter. Shorter ignition delay times were seen with an increase in changing θ. The mixture variations are necessary to observe trends in the ignition behavior under real world conditions where combustor could be operating over wide ranges of settings. The experimental data was compared with two combustion chemical kinetic mechanisms GRI-Mech v3.0 and AramcoMech v2.0. In general, these models did not accurately predict the ignition delay time, but generally predicted the trends seen in parametric variations in T, ϕ, etc. In addition, high-speed imaging of the experiments was taken at the end wall of the shock tube to compare with different methods of determining the ignition delay time. The high-speed camera images revealed insights into the non-homogeneity of the combustion events within the shock tube for large CO_2 dilutions, but had some shortcomings to be addressed in future work.

The data suggests that there is a significant limit to the models at predicting the ignition delay time of syngas with variations in compositions with high dilutions of CO_2. Current experiments were performed around 1.7 atm. More analysis must be done at higher pressures to evaluate the effects of CO_2 within the entire range of operating conditions of a sCO_2 combustor. In addition, modifications for the camera must be added in order to observe light at a lower

wavelength. Present data would serve as crucial validation steps needed for the development and refinement of future combustion kinetic models.

REFERENCES

[1] McClung, A., 2016, "Oxy-Combustion Integration for Direct Fired sCO2 Cycles," The 5th Intl Symposium - Supercritical CO2 Power CyclesSan Antonio, TX.

[2] Fetvedt, J., "8Rivers Development Of The sCO2 Allam Cycle 50MWth Demonstration Plant," Proc. The 5th International Symposium - Supercritical CO2 Power Cycles.

[3] Chiesa, P., Lozza, G., and Mazzocchi, L., 2005, "Using Hydrogen as Gas Turbine Fuel," Journal of Engineering for Gas Turbines and Power, 127(1), pp. 73-80.

[4] Kéromnès, A., Metcalfe, W. K., Heufer, K. A., Donohoe, N., Das, A. K., Sung, C.-J., Herzler, J., Naumann, C., Griebel, P., Mathieu, O., Krejci, M. C., Petersen, E. L., Pitz, W. J., and Curran, H. J., 2013, "An experimental and detailed chemical kinetic modeling study of hydrogen and syngas mixture oxidation at elevated pressures," Combustion and Flame, 160(6), pp. 995-1011.

[5] Walton, S. M., He, X., Zigler, B. T., and Wooldridge, M. S., 2007, "An experimental investigation of the ignition properties of hydrogen and carbon monoxide mixtures for syngas turbine applications," Proceedings of the Combustion Institute, 31(2), pp. 3147-3154.

[6] Vasu, S. S., Davidson, D. F., and Hanson, R. K., 2011, "Shock Tube Study of Syngas Ignition in Rich CO2Mixtures and Determination of the Rate of H + O2+ CO2→ HO2+ CO2," Energy & Fuels, 25(3), pp. 990-997.

[7] Thi, L. D., Zhang, Y., and Huang, Z., 2014, "Shock tube study on ignition delay of multi-component syngas mixtures – Effect of equivalence ratio," International Journal of Hydrogen Energy, 39(11), pp. 6034-6043.

[8] Petersen, E. L., Kalitan, D. M., Barrett, A. B., Reehal, S. C., Mertens, J. D., Beerer, D. J., Hack, R. L., and McDonell, V. G., 2007, "New syngas/air ignition data at lower temperature and elevated

pressure and comparison to current kinetics models," Combustion and Flame, 149(1-2), pp. 244-247.

[9] Koroglu, B., Pryor, O. M., Lopez, J., Nash, L., and Vasu, S. S., 2016, "Shock tube ignition delay times and methane time-histories measurements during excess CO2 diluted oxy-methane combustion," Combustion and Flame, 164, pp. 152-163.

[10] Koroglu, B., Pryor, O., Lopez, J., Nash, L., and Vasu, S. S., 2015, "Methane Ignition Delay Times in CO2 Diluted Mixtures in a Shock Tube," 51st AIAA/SAE/ASEE Joint Propulsion Conference, American Institute of Aeronautics and Astronautics AIAA 2015-4088.

[11] Smith, G. P., Golden, D. M., Frenklach, M., Moriarty, N. W., Eiteneer, B., Goldenberg, M., Bowman, C. T., Hanson, R. K., Song, S., and Gardiner Jr, W. C., 1999, "GRI-Mech 3.0," URL: http://www.me.berkeley.edu/gri_mech, 51, p. 55.

[12] A.G. Gaydon, I. R. H., 1963, The shock tube in high-temperature chemical physics, Reinhold, New York.

[13] Koroglu, B., and Vasu, S. S., 2016, "Measurements of Propanal Ignition Delay Times and Species Time Histories Using Shock Tube and Laser Absorption," International Journal of Chemical Kinetics.

[14] Pryor, O., Barari, G., Koroglu, B., Lopez, J., Nash, L., and Vasu, S. S., 2016, "Shock Tube Ignition Studies of Advanced Biofuels," 52nd AIAA/SAE/ASEE Joint Propulsion Conference, American Institute of Aeronautics and Astronautics AIAA 2016-4691.

[15] Koroglu, B., Pryor, O., Lopez, J., Nash, L., and Vasu, S. S., 2016, "Shock Tube Ignition and CH4 Time-Histories during Propanal Oxidation," 54th AIAA Aerospace Sciences Meeting, American Institute of Aeronautics and Astronautics AIAA 2016-0179.

[16] Davidson, D. F., and Hanson, R. K., 2004, "Interpreting shock tube ignition data," International Journal of Chemical Kinetics, 36(9), pp. 510-523.

[17] Atkinson, R., Perry, R. A., and Pitts Jr., J. N., 1977, "Absolute rate constants for the reaction of OH radicals with allene, 1,3-butadiene, and 3-methyl-1-butene over the temperature range 299–424 °K," J. Chem. Phys., 67, p. 3170.

[18] Pryor, O. M., Barak, S., Koroglu, B., Ninnemann, E., and Vasu, S., 2017, "Measurements and interpretation of shock tube ignition delay times in highly CO2 diluted mixtures using multiple diagnostics," Combustion and Flame, 180, pp. 67-76.

[19] Gaydon, A. G., 1974, "The Carbon Monoxide Flame," The Spectroscopy of Flames, Springer Netherlands, Dordrecht, pp. 127-143.

[20] "Phantom V21x Color and Spectral Response Curve."

[21] Liu, F., Guo, H., and Smallwood, G. J., 2003, "The chemical effect of CO2 replacement of N2 in air on the burning velocity of CH4 and H2 premixed flames," Combustion and Flame, 133(4), pp. 495-497.

[22] Ninnemann, E., Pryor, O., Barak, S., Koroglu, B., Sosa, J., Ahmed, K., and Vasu, S., 2017, "High-Speed Imaging of the Dynamics of H2/O2 Ignition at Low to Moderate Temperatures in a Shock Tube," 55th AIAA Aerospace Sciences Meeting, American Institute of Aeronautics and Astronautics AIAA 2017-1796.